

Effect of conical intersection of benzene on non-adiabatic dynamics

Duo-Duo Li(李多多) and Song Zhang(张嵩)

Citation: Chin. Phys. B, 2022, 31 (**8**): 083103. DOI: 10.1088/1674-1056/ac5607
Journal homepage: http://cpb.iphy.ac.cn; http://iopscience.iop.org/cpb

What follows is a list of articles you may be interested in

Quantum and quasiclassical dynamics of C($^{3} P$) + H$_{2}(^{1} \varSigma_{\text{g}}^+)\rightarrow H(^{2} S)$ + CH($^{2} \varPi$) reaction: Coriolis coupling effects and stereodynamics

Dong Liu(刘栋), Lulu Zhang(张路路), Juan Zhao(赵娟), Qin Zhang(张芹), Yuzhi Song(宋玉志), and Qingtian Meng(孟庆田)
Chin. Phys. B, 2022, 31 (**4**): 043102. DOI: 10.1088/1674-1056/ac3989

Plasticity and melting characteristics of metal Al with Ti-cluster under shock loading

Dong-Lin Luan(栾栋林), Ya-Bin Wang(王亚斌), Guo-Meng Li(李果蒙), Lei Yuan(袁磊), and Jun Chen(陈军)
Chin. Phys. B, 2021, 30 (**7**): 073103. DOI: 10.1088/1674-1056/abe1a0

State-to-state dynamics of reactions H+DH'(v = 0,j = 0) → HH'(v',j')+D/HD(v',j')+H' with time-dependent quantum wave packet method

Juan Zhao(赵娟), Da-Guang Yue(岳大光), Lu-Lu Zhang(张路路), Shang Gao(高尚), Zhong-Bo Liu(刘中波), and Qing-Tian Meng(孟庆田)
Chin. Phys. B, 2021, 30 (**7**): 073102. DOI: 10.1088/1674-1056/abf559

Size effect of He clusters on the interactions with self-interstitial tungsten atoms at different temperatures

Jinlong Wang(王金龙), Wenqiang Dang(党文强), Daping Liu(刘大平), Zhichao Guo(郭志超)
Chin. Phys. B, 2020, 29 (**9**): 093101. DOI: 10.1088/1674-1056/ab9619

Mechanism analysis of reaction $S^{+}(^{2}D)+H_{2}(X^{1}\Sigma_{g}^{+})\rightarrow SH^{+}(X^{3}\Sigma^{-})+H(^{2}S)$ based on the quantum state-to-state dynamics

Jin-Yu Zhang(张金玉), Ting Xu(许婷), Zhi-Wei Ge(葛志伟), Juan Zhao(赵娟), Shou-Bao Gao(高守宝), Qing-Tian Meng(孟庆田)
Chin. Phys. B, 2020, 29 (**6**): 063101. DOI: 10.1088/1674-1056/ab889c

---

Effect of conical intersection of benzene on non-adiabatic dynamics

Duo-Duo Li(李多多)[1,2] and Song Zhang(张嵩)[1,2,†]

[1] *State Key Laboratory of Magnetic Resonance and Atomic and Molecular Physics, Innovation Academy for Precision Measurement Science and Technology, Chinese Academy of Sciences, Wuhan* 430071, *China*
[2] *University of Chinese Academy of Sciences, Beijing* 100049, *China*

(Received 7 December 2021; revised manuscript received 5 February 2022; accepted manuscript online 17 February 2022)

The effect of conical intersection on the excited dynamics of benzene is studied by *ab initio* theory of electronic structure, which provides an important insight into photophysical and photochemical reactions. Based on the CASSCF(6,6)/6-31+G(d, p) method, the topological structures of conical intersections S_1/S and S_2/S_1 of benzene, as well as the optimal structures of the ground state (S) and excited states (S_1, S_2), are determined. The energy minima of the S_1 state and S_2 state are estimated at 4.608 eV and 6.889 eV, respectively. In addition, the energy values of the conical intersections of S_1/S and S_2/S_1 are predicted to be 5.600 eV and 6.774 eV. According to the topological structures and energy values of the S_2/S_1 and S_1/S conical intersections, the photophysical behavior of benzene excited to the S_2 state and the effects of the S_2/S_1 and S_1/S conical intersections are discussed in detail.

Keywords: conical intersection, nonadiabatic dynamics, ultrafast relaxation, quantum chemical calculations

PACS: 31.50.Gh, 31.15.xv, 31.70.Hq, 31.15.vq **DOI:** 10.1088/1674-1056/ac5607

1. Introduction

Born–Oppenheimer (BO) approximation is one of the fundamental approximations of atomic and molecular physics.[1] In the BO approximation, the electron and nuclear wave functions are separable because of their different time scales of motion, which makes up the premise for the adiabatic description of chemical reactions.[2] However, the BO approximation loses its effectiveness in some processes, such as ultrafast non-radiative relaxation, photodissociation, photofragmentation, chemiluminescence or isomerization of polyatomic molecules, *etc*.[3–6] For chemical reactions that occur in electronically excited states, non-adiabatic transition,[7–9] that is, the coupling between two close-lying adiabatic surfaces caused by nuclear motion is not only universal but also essential in many chemical processes and biological processes. In particular, the conical intersection (CI), in which two adiabatic surfaces cross in at least the two-dimensional coordinate, is accepted widely as the dynamic funnel for such non-adiabatic transitions.[10–13] Conical intersection plays a significant role in nonadiabatic dynamic behavior in terms of molecular structure and chemical reactivity.[14–17]

Benzene is selected for this study because although it has been studied extensively over many years, there are still some uncertainties regarding the dynamics. Owing to the ability to detect chemical behavior on a much shorter time scale, researches concentrate on the dynamic properties of benzene and its derivatives, such as its fluorescence lifetime, excited state relaxation, and photolysis.[18–30] It is noticed early that the fluorescence quantum yield of benzene drops sharply as the excitation energy is 3000 cm^{-1} above the 0–0 transition energy of the S_1 state. This phenomenon has been explained by the effect of a CI between the S and S_1 states, which can promote non-radiative relaxation between electronic states. The lifetimes of vibronic sequence v_6 and v_7 in the $^1B_{2u}$ state were reported on a time scale of nanoseconds. Furthermore, the possible photochemical reactions caused by the effects of the S_2/S_1 and S_1/S conical intersections were inspected based on the MC-SCF calculations.[20] It is demonstrated that the occurrence of Dewar benzene as a product of the S_2 photochemistry is directly attributed to the efficient crossing via the conical intersection of S_2/S_1. Moreover, the origin of the low quantum yield (~ 0.02) of photochemical benzvalene production from the S_1 results from the fact that most of populations decay and return to S benzene via S_1/S conical intersection. Furthermore, the rapid decay of the S_2 state was measured to be about 50 fs by using time-resolved time-of-flight mass spectrometry and photoelectron spectroscopy experimentally.[31–35] Moreover, the arrival times of the wavepacket from the S_2 state to the S_1 and S states are 64 fs and 68 fs by VUV time-resolved photoelectron spectra, respectively.[36] It is considered that most of the populations in the S_2 state decay directly to the S state and are not detected in the S_1 state. And it is also pointed out that a small number of the populations do get trapped in the S_1 state and the conversion of the S_2 state into the S_1 state is only about 1%,[33,34] while the yield of $S_2 \rightarrow S_1$ estimated from the time-resolved photoelectron imaging is much greater than 10%.[31] In addition, the long lifetime of the S_1 state conversion into the S state was measured to be 6.5, 6.7, and 7.6 ps given in

†Corresponding author. E-mail: zhangsong@wipm.ac.cn
© 2022 Chinese Physical Society and IOP Publishing Ltd

Refs. [31–35], respectively. Furthermore, the excited state direct dynamic behaviors in the S_2 state and the S_1 state with quantum calculations were illustrated, and the mechanisms of internal conversion were revealed. It is concluded that the relaxation of the S_2 state is very fast via the S_2/S_1 intersection and the following population on the S_1 state decays much more slowly via the S_1/S intersection. The precise branching ratio between the populations in the two excited states would require a more detailed investigation of the topological geometries.

In this work, the energy values, structures, and orbits of the ground state and the excited states are determined by using the multi-configuration complete active space self-consistent field (CASSCF) theory.[37] At the same time, the topological structures and energy values of the S_2/S_1 and S_1/S conical intersections are also obtained. These results are conducive to explaining and clarifying the photophysical behavior of benzene excited to the S_2 state and the effects of the S_2/S_1 and S_1/S conical intersections.

2. Calculation methods

The photochemical dynamics of benzene have a high degree of multi-configuration due to the multiple electronic states with many degeneracies and near degeneracies due to the presence of conical intersection. The CASSCF methods were employed to study the relaxation path of the excited states of benzene. The static electronic structure calculation was carried out by the CASSCF(6, 6) method with the basis set 6-31+G(d, p) through using Gaussian 09 software.[38] In order to clarify the relaxation process of the $\pi\pi^*$ excited state, it is necessary to select the π characteristic orbits and exchange the n orbit of HOMO-2 [the highest occupied molecular orbit (HOMO)] with the π orbits of HOMO-4. The final activation space is composed of six electrons and six orbits (*i.e.*, three π orbits and three π^* orbits). The energy values, structures, and the orbit of the ground state and orbits of the excited states are calculated. Finally, the CIs of S_2/S_1 and S_1/S are determined by scanning along the C1–C2–C3–C6 dihedral angle, and the structures, energy values, and orbits are all obtained. Moreover, the energy values of some critical points are obtained based on the CASPT2 method with the same basis set.

3. Results and discussion

The geometries of the ground state and excited states are optimized by the CASSCF(6, 6) method with the 6-31+G(d, p) basis set and illustrated in Fig. 1. The optimized structures of the S_0, S_1, and S_2 states are all planar with D_{6h} symmetry. The length of C–C bond and C–H bond in the S_0 state are calculated to be 1.398 Å and 1.076 Å at the CASSCF(6, 6)/6-31+G(d, p), respectively. And the C–C bond lengths of the S_0 state are calculated to be 1.394, 1.37, and 1.39 Å by the methods of RASSCF(6, 1+5+6)/6-31G(d), CASSCF(6, 6)-PT2/6-31G(d), and CASSCF(6, 5)/6-31G(d), respectively.[39,40] In addition, according to the calculation by the CASSCF(6, 6)/6-31+G(d, p) method, the length of the C–C bond and C–H bond of the S_1 state are 1.435 Å and 1.074 Å, respectively. And based on the calculations by the methods of RASSCF(6, 1+5+6), CASSCF (6, 6)-PT2/6-31G(d), and CASSCF(6, 5)/6-31G(d), the C–C bond lengths of the S_1 state are determined to be 1.432, 1.43, and 1.47 Å, respectively.[39,40] The calculated geometry of the S_0 state and the S_1 state are in agreement with the previous results. However, two different structures of the S_2 state, *i.e.*, a boat-shaped and a plane structures, are discovered with the RASSCF(6, 1+5+6)/6-31G(d) and SCF/4-31G[39,41] It is interesting that three minima at the S_2 state were also mentioned by employing the RASSCF method.[30] However, our calculations confirm that a plane geometry is more stable, which is consistent with the previous planar structure.[39] In addition, the C–C bond length of the S_2 state is also consistent with the values of 1.415 Å and 1.414 Å calculated by the CASSCF(6, 6)/6-31+G (d, p) method and RASSCF(6, 1+5+6)/6-31G(d) method, respectively.[39]

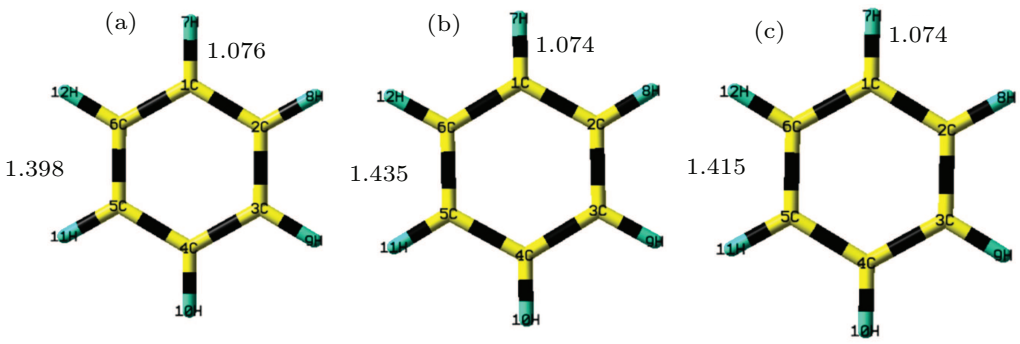


Fig. 1. Optimized geometries of (a) ground state S_0, (b) the first excited state S_1, and (c) the second excited state S_2 based on CASSCF(6, 6)/6-31+G(d, p). Bond lengths are all in unit Å.

Figure 2 shows the six selected orbits. The HOMO-2 to HOMO orbit and the LUMO [the lowest unoccupied molecular orbit (LUMO)] to LUMO+2 orbit are π orbit and π^* orbit, respectively. The excited states S_1 and S_2 are both optically bright $\pi\pi^*$ state. The S_1 state is predominantly a transition from the e_{1g} orbit to the e_{2u} orbit, while the S_2 state arises from the transition from the e_{1g} orbit to the e_{2u} orbit.

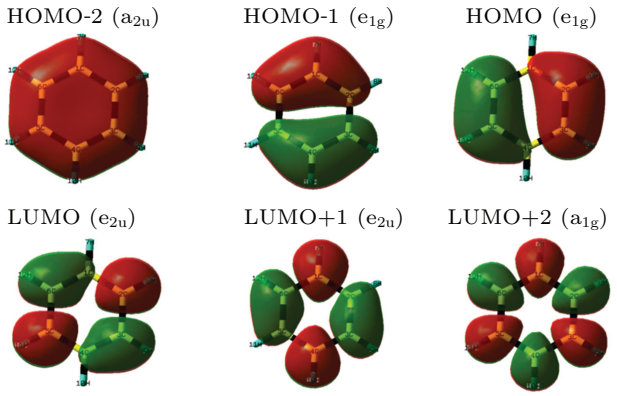


Fig. 2. Six selected orbits: π obits (upper), and π^* orbits (lower).

The adiabatic excited energy values of S_1 and S_2 states are calculated to be 4.608 eV and 6.889 eV, respectively. And the vertical energy values of the S_1 state with 5.020 eV and 4.755 eV obtained by the CASSCF(6,6)/6-311G+(d, p) method and the CASPT2/6-311G+(d, p) method. The vertical energy values of the S_2 state obtained by the CASSCF(6,6)/6-311G+(d, p) method and the CASPT2/6-311G+(d, p) method are both 7.307 eV. The previous experimental values of the S_1 state are measured to be 4.722,[42] 4.75,[31,33] and 4.9 eV.[40,43] Simultaneously, the energy values of the S_2 state are measured to be 6.05 eV[33,44] and 6.2 eV.[39,40] Based on the different methods, the energy values of the two excited states are summarized in Table 1. Our result of the S_1 state is slightly lower than the other calculations but closer to the experimental values. However, the energy values of the S_2 state are 6.159 eV and 6.537 eV obtained by the method of PBE1PBE/6-311G++(3df, 3dp)[45] and the calculations by the method of CCSD/aug-cc-pVTZ-CM2[46] are closer to the experimental values. The results of the S_2 state, calculated by the CASSSCF method,[37] are obviously higher than the experimental values. Since dynamic electron correlation effects are not considered, the higher excited state energy values calculated by the CASSCF method are different form the experimental values. While the vertical excitation energy values obtained at the CCSD and the CASPT2 levels are slightly lower than the values obtained by the CASSCF method and closer to the experimental value since the dynamic electron correlation effect is taken into consideration in the first two methods mentioned above.

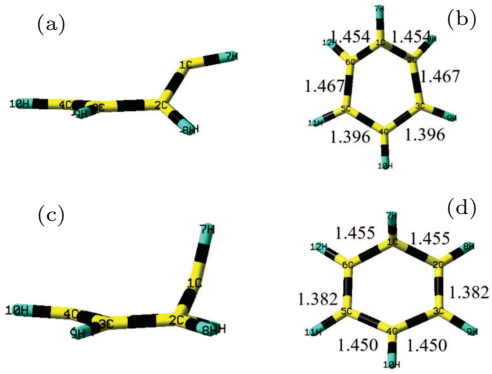


Fig. 3. (a) Side view and (b) top view of optimized structure of S_1/S_0 conical intersection, (c) side view and (d) top view of optimized S_2/S_1 conical intersection. Bond lengths are in unit Å.

Table 1. Measured and calculated energy values (in unit eV) of excited states of benzene.

State	$E_{expt.}$	$E_{adiabatic}$	$E_{vertical}$					
		CASSCF(6, 6)/6-31+G(d, p)	CASSCF(6, 6)/6-31+G(d, p)	CASPT2/6-31+G(d, p)	CASSCF(6, 5)/6-31G(d)[40]	CASSCF(6, 6)/6-31G(d)[40]	PBE1PBE/6-311G++(3df, 3dp)[45]	CCSD/aug-cc-pVTZ-CM2[46]
S_1	4.75[31,33] 4.9[40,42] 4.722[41]	4.608	5.020	4.755	6.02	5.09	5.499	5.192
S_2	6.05[33,34] 6.2[39,40]	6.889	7.307	7.307	7.63	8.28	6.159	6.537

The optimal structures at the CIs of S_1/S_0 and S_1/S_2 are shown in Fig. 3, and the detailed parameters of the bond distances, the bond angles and the dihedral angles are listed in Table 2. Our calculations reveal that the configures at the CIs of S_2/S_1 and S_1/S_0 no longer remain planar but evolves a half-boat-shaped structure along the out-of-plane coordinates. The distances of C2$\cdots$C6 and C3$\cdots$C5 bonds of the S_1/S are 1.931 Å and 2.327 Å, respectively. And the C1–C2–C3–C6 and C4–C5–C6–C3 dihedral angles are 45.82° and 3.894°, respectively. The structure shape of S_1/S_0 is similar to the previous calculated results.[26,40,44,47] According to the previous results, the distances of C2$\cdots$C6 and C3$\cdots$C5 were reported to be 1.92 Å and 2.33 Å by the method of CASPT2 and CASSCF(6, 5) with the 6-31G(d) basis set, respectively. The energy of the optimized structure at the CI of S_1/S_0 is predicted to be 5.600 eV by the CASSCF method. It is only 0.992 eV higher than the minimum energy of the S_1 state. The energy at the CI of S_1/S is determined to be 5.395 eV by the CASPT2 method, which is 0.205 eV lower than the value by the CASSCF method. Although the structures of the S_2/S_1 are a boat-shape structure obtained by the CASSCF(6, 6)/6-31G(d) and CASSCF(6, 5)/6-31G(d) methods, our calculated

structure of the S_2/S_1 is confirmed to be a half-boat-shaped structure. The same structure is identified by the the method of RASSCF(6, 1+5+6)/6-31G(d). The C2···C6 and C3···C5 bond distances of S_2/S_1 are 2.443 Å and 2.488 Å, respectively. The C1–C2–C3–C6 and C4–C5–C6–C3 dihedral angles are 29.68° and 10.29°. In addition, the distances of C2···C6 and C3···C5 are about 2.46 Å and 2.49 Å at CASPT2/6-31G(d) and CASSCF(6, 5)/6-31G(d), respectively.[30] The bond distances C2···C6 and C3···C5 of the S_1/S_0 are determined to be 1.931 Å and 2.327 Å, respectively, while the C2.C6 and C3.C5 bond distances of the S_2/S_1 are determined to be 2.443 Å and 2.488 Å. It is concluded that the structure of the S_2/S_1 becomes more slightly enlarged than that of the S_1/S_0 and the warping degree of the S_2/S_1 is not larger than that of S_1/S_0. The energy of the optimal CI of the S_2/S_1 is located at 6.774 eV by the CASSCF method. It is obviously 1.174 eV higher than the energy of the S_1/S_0. The energy at the CI of S_2/S_1 determined by the CASPT2 method is 6.590 eV, 0.184 eV lower than that on the CASSCF method. With the half-boat-shaped the structure formed, the molecules lose their planar structures and their orbitals also change simultaneously. The corresponding orbitals of the S_1/S and S_1/S_2 are shown in Fig. 4, respectively. Since the coupling of the orbitals occurs in the evolution of the relaxation, the orbital is no longer as regular as the shape in the Frank–Condon region. It is inferred that the changes in orbital properties of CIs are due to the reduced symmetry of D_{6h} and the coupling of states.

Table 2. Optical CIs (S_1/S_0 and S_2/S_1) structural parameters. Bond distances are in unit Å, and bond and dihedral angles are in degree.

	S_1/S	S_2/S_1
C2···C6	1.931	2.443
C3···C5	2.327	2.488
H7–C1–C2	120.4	122.1
C1–C2–C3	120.4	106.1
C3–C4–C5	112.9	118.5
C6–C1–C2	83.2	114.5
C1–C2–C3–C6	45.8	29.9
C2–C3–C4–C5	7.0	20.5
C1–C2–C3–C4	41.9	19.4
C4–C5–C6–C3	3.9	10.3

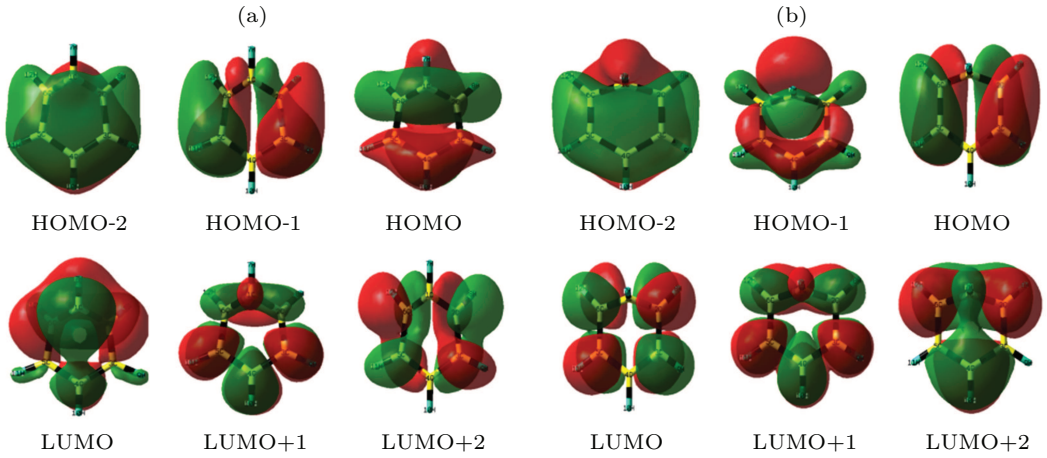


Fig. 4. Orbits of (a) S_1/S_0 and (b) S_2/S_1 conical intersections.

Time-resolved time-of-flight mass spectrometry and photoelectron spectroscopy experiments reveal that the relaxed lifetimes of S_2 and S_1 states are reported to be 50 fs and 6.7 ps, respectively.[31–35] Further, through the vacuum ultraviolet time-resolved photoelectron spectrum, the arrival times of S_2 at S_1 and S states are 64 fs and 68 fs, respectively,[36] which shows that the relaxation time of the S_1 state is very short. These experiments indicate that the decay of the S_2 state is so fast. Our calculations show that the S_2/S_1 conical intersection is located at the out-of-plane bent structure near the minimum–energy structure of S_2. The energy values of the S_2 state and the CI of the S_2/S_1 are 6.889 eV and 6.774 eV, respectively. Since the energy value of the S_2 state is 0.115 eV higher than the energy value of the S_2/S_1, there is no potential barrier from the S_2 state to the S_2/S_1. This could explain that the relaxation process occurs on an ultrafast time scale with a lifetime of 50 fs after the excitation of the S_2 state, which is consistent with previous result. Reparameterization of PM3-FOMO-CASCI (6/6) predicts that the S_2 state decays to the lower excited states through CIs in a time of less than 100 fs.[40] It is mentioned that the different relaxation pathways are reported following the relaxation of the S_2 state. As described above, the CIs of the S_2/S_1 and S_1/S are both half-boat-shaped structures. It results in the fact that the wave packet will pass through the second CI immediately once passing S_2/S_1 without undergoing significant structural changes. Simultaneously, since the energy value of the CI of the S_2/S_1 is obviously 1.174 eV higher than the S_1/S_0, the large energy gradient will promote the direct internal conversion into the S_0 state. Although the direct relaxation to the S_0 state dominants, the branching ratio of at least 1% from S_2 to S_1 state is still indicated.[33,34] Specially, the yield of $S_2 \rightarrow S_1$ is estimated at a value much greater than 10% by time-resolved photoelectron imaging with a time resolution of

22 fs.[31] Our calculations show that the energy difference between S_2/S_1 and the minimum point of the S_1 state is as high as 2.166 eV. The high excess energy will preferentially make wave packet transfer to the minimum of the S_1 state. Furthermore, the energy of S_1/S_0 is only 0.992 eV higher than the minimum energy of the S_1 state. Following arriving at a minimum value of the S_1 state, the wave packet carrying the excess energy overcomes the lower potential barrier and decays to the S_0 state through the CI of S_1/S_0. Furthermore, since the geometry changes from a planar structure on the S_1 minimum point to a half-ship structure of S_1/S_0, the indirect relaxation to the S_0 state is slow along multiple CIs paths. Accurately, the long lifetime decay of the S_1 state to the S_0 state is observed in the experiment. It is unfortunate that the quantum yields of the relaxation channels cannot be obtained in the present calculations.

4. Conclusions

The multi-configuration complete active space self-consistent field method of the excited states of benzene provides important insights into the internal conversion mechanism. Based on the CASSCF(6, 6) method with 6-31+G(d, p) basis set, the minimum–energy structures of S, S_1, and S_2 states are optimized to be planar structures. The adiabatic energy values of the S_1 and S_2 states are estimated at 4.608 eV and 6.889 eV, respectively. Simultaneously, optimized structures of the CIs S_1/S and S_2/S_1 are both half-boat structures. Although the structures of CIs S_1/S and S_2/S_1 are similar, the structure of S_1/S is narrower and more warped than that of S_2/S_1. The energy values of S_1/S and S_2/S_1 are predicted to be 5.600 eV and 6.774 eV, respectively. Owing to the small difference in energy and the similar structures between the conical intersections of S_2/S_1 and S_1/S, wave packet directly decays to the S state through the two CIs after the excitation of the S_2 state. And this relaxation proves to be dominant. Our calculations also pointed out that a small fraction of wave packet relaxes to a minimum value of planar S_1 state through the CI of S_2/S_1. The subsequent wave packets with excess energy can cross the barrier of the CI of S_1/S of the S_1 state. It takes longer time for the geometry to change from the planar minimum structure of the S_1 state to the CI of S_1/S_0.

Acknowledgements

Project supported by the National Key Research and Development Program of China (Grant No. 2019YFA0307700) and the National Natural Science Foundation of China (Grant Nos. 11974381, 11674355, and 21773299).

References

[1] Born M and Oppenheimer R 1927 *Ann. Phys.-Berlin.* **389** 457
[2] Lim J S and Kim S K 2010 *Nat. Chem.* **2** 627
[3] Yarkony D R 1996 *Rev. Mod. Phys.* **68** 985
[4] Worth G A and Cederbaum L S 2004 *Ann. Rev. Phys. Chem.* **55** 127
[5] Mukherjee B, Ghosh S, Adhikari S and Iop 2018 *J. Phys. Conf. Ser.* **1148** 012001
[6] Koppel H, Domcke W and Cederbaum L S 1984 *Adv. Chem. Phys.* **57** 59
[7] Yang J, Zhu X L, Wolf T J A, *et al.* 2018 *Science* **361** 64
[8] Tully J C 2012 *J. Chem. Phys.* **137** 22A301
[9] Jasper A W, Nangia S, Zhu C Y and Truhlar D G 2006 *Acc. Chem. Res.* **39** 101
[10] Yoon J H, Woo K C and Kim S K 2014 *Phys. Chem. Chem. Phys.* **16** 8949
[11] Xie C J, Malbon C L, Yarkony D R, Xie D Q and Guo H 2018 *J. Am. Chem. Soc.* **140** 1986
[12] Klessinger M 1995 *Angew. Chem. Int. Ed.* **34** 549
[13] Horio T, Fuji T, Suzuki Y I and Suzuki T 2009 *J. Am. Chem. Soc.* **131** 10392
[14] Zgrablic G, Novello A M and Parmigiani F 2012 *J. Am. Chem. Soc.* **134** 955
[15] Woo J K, Jang J E, Kang J H, *et al.* 2017 *Mol. Cancer Ther.* **16** 1355
[16] Levine B G and Martinez T J 2007 *Annu. Rev. Phys. Chem.* **58** 613
[17] Han S, Lim J S, Yoon J H, *et al.* 2014 *J. Chem. Phys.* **140** 054307
[18] Malar E J P and Jug K 1984 *J. Phys. Chem.* **88** 3508
[19] Matos J M O, Roos B O and Malmqvist P A 1987 *J. Chem. Phys.* **86** 1458
[20] Palmer I J, Ragazos I N, Bernardi F, Olivucci M and Robb M A 1993 *J. Am. Chem. Soc.* **115** 673
[21] Sponer J, Cejka J and Wichterlova B 1998 *J. Phys. Chem. B* **102** 7169
[22] Yoon B, Sheaff C N, Eastwood D and Wai C M 2007 *J. Nanophoton.* **1** 013508
[23] Okada T, Yamanaka K, Goto Y and Inagaki S 2008 *Pol. J. Chem.* **82** 729
[24] Zhang C, Allotta P M, Xiong G and Stair P C 2008 *J. Phys. Chem. C* **112** 14501
[25] Chakraborty S, Omidyan R, Alata I, *et al.* 2009 *J. Am. Chem. Soc.* **131** 11091
[26] Li Q S, Mendive-Tapia D, Paterson M J, *et al.* 2010 *Chem. Phys.* **377** 60
[27] Liu Y Z, Tang B F, Shen H, Zhang S and Zhang B 2010 *Opt. Express* **18** 5791
[28] Galbraith M C E, Scheit S, Golubev N V, *et al.* 2017 *Nat. Commun.* **8** 1018
[29] Johnson P M 2020 *J. Chem. Phys.* **152** 134307
[30] Varras P C, Gritzapis P S and Siskos M G 2020 *ChemistrySelect* **5** 2810
[31] Suzuki Y, Horio T, Fuji T and Suzuki T 2011 *J. Chem. Phys.* **134** 184313
[32] Suzuki T 2012 *Int. Rev. Phys. Chem.* **31** 265
[33] Radloff W, Stert V, Freudenberg T, *et al.* 1997 *Chem. Phys. Lett.* **281** 20
[34] Radloff W, Freudenberg T, Ritze H H, *et al.* 1996 *Chem. Phys. Lett.* **261** 301
[35] Yin S H, Liu H P, Zhang J Y, *et al.* 2003 *Chin. J. Chem. Phys.* **16** 171
[36] Adachi S and Suzuki T 2020 *Phys. Chem. Chem. Phys.* **22** 2814
[37] Roos B O 1987 *Adv. Chem. Phys.* **69** 399
[38] Frisch M J, Trucks G W, Schlegel H B, *et al.* Gaussian 09 Rev. B.01. Wallingford, CT, 2009
[39] Thompson A L and Martinez T J 2011 *Faraday Discuss.* **150** 293
[40] Toniolo A, Thompson A L and Martínez T J 2004 *Chem. Phys.* **304** 133
[41] Meisl M and Janoschek R 1986 *J. Chem. Soc. Chem. Commun.* 1066
[42] Bieri G, Asbrink L and Vonniessen W 1981 *J. Electron Spectros. Relat. Phenomena* **23** 281
[43] Lorentzon J, Malmqvist P A, Fulscher M and Roos B O 1995 *Theor. Chim. Acta* **91** 91
[44] Lasorne B, Bearpark M J, Robb M A and Worth G A 2008 *J. Phys. Chem. A* **112** 13017
[45] Studzinski H, Zhang S, Wang Y and Temps F 2008 *J. Chem. Phys.* **128** 164314
[46] Christiansen O, Koch H, Halkier A, *et al.* 1996 *J. Chem. Phys.* **105** 6921
[47] Smith B R, Bearpark M J, Robb M A, Bernardi F and Olivucci M 1995 *Chem. Phys. Lett.* **242** 27